closely related, this procedure resulted in a conservative test. Sequences examined in *P. crassifolia* were sequences PcS1–9, PcS11–13, PcS16, and PcS20–22.
18. Tests for positive Darwinian selection (an excess of P_n relative to P_s) were performed using the approach of Nei and Jin (*32*) as implemented in MEGA (*33*). DNA sequences used in this analysis have been deposited in GenBank [accession numbers L40539 to L40551 (*15*) and L46653 to L46680 (*6*)]. Evidence for positive selection may be obscured by the accumulation of neutral mutations when more distantly related alleles are compared. Accordingly, P_n and P_s (and their SEs) were calculated separately for each major clade of *P. crassifolia* alleles (Fig. 3). To maximize the number of sequences analyzed, we used sequence data corresponding to residues 1 through 59 (Fig. 1). This region contains the two hypervariable regions (*7*), which may play a role in specificity determination. For the large clade of alleles from *P. crassifolia* (sequences 1 to 19 and 24 to 28), the mean values (with SEs) were P_n = 0.3082 (0.0227) and P_s = 0.2278 (0.0411); P_n/P_s = 1.47 ($P < 0.05$, one-tailed). For the small *P. crassifolia* clade (sequences 20 to 23), P_n = 0.2489 (0.0308) and P_s = 0.1855 (0.0569); P_n/P_s = 1.41 (not significant). For the four closely related alleles in *S. carolinense* (ScS1, ScS10, ScS11, and ScS13; see Fig. 3), P_n = 0.1214 (0.0296) and P_s = 0.0581 (0.0296); P_n/P_s = 2.09 [$P < 0.05$, one-tailed; see also (*14*)]. Comparisons among the remaining nine more distantly related *S. carolinense* alleles showed no excess of P_n [P_n = 0.4916 (0.0293), P_s = 0.5495 (0.0599); P_n/P_s = 0.89 (not significant)], similar to values found when comparisons were made across the two clades of alleles in *P. crassifolia* (P_n/P_s = 0.90).
19. A. G. Clark and T.-h. Kao, *Proc. Natl. Acad. Sci. U.S.A.* **88**, 9823 (1991).
20. K. Hinata, M. Watanabe, S. Yamakawa, Y. Satta, A. Isogai, *Genetics* **140**, 1099 (1995).
21. R. G. Olmstead and J. A. Sweere, *Syst. Biol.* **43**, 467 (1994).
22. N. Takahata, *Mol. Biol. Evol.* **10**, 2 (1993).
23. In calculating the probability $g_{nk}(t)$ that, given a sample of n extant alleles, they coalesced into k lineages t generations ago, it is convenient to replace t by t', defined as

$$t' = \frac{t}{2N_e f_s} \quad (7)$$

(*9*), where f_s is a scaling factor specific to frequency-dependent selection at the *S* locus, defined as

$$f_s = \frac{\sqrt{2}}{16N^2 va(J - v/a)^2} \quad (8)$$

(*10*), where v, J, and a are defined as in (*16*). The probability $g_{nk}(t')$ is then

$$g_{nk}(t') = \sum_{m=k}^{n} \frac{(2m-1)(-1)^{m-k} k_{(m-1)} n_{[m]}}{k!(m-k)! n_{(m)}} \exp\left[-\frac{m(m-1)t'}{2}\right] \quad (9)$$

for $2 \le k \le n$, where $n_{[m]} = n(n-1)(n-2)\ldots(n-m+1)$, $n_{(m)} = n(n+1)(n+2)\ldots(n+m-1)$, and m is a variable changing from k to n (*9*). For a given origination rate, we then calculate the probability $g_{nk}(t')$ to find the value of t' that maximizes the probability of observing n and k. The value of N_e associated with the ML estimate of t' is then obtained from Eq. 7 using $t = 15 \times 10^6$, assuming that *Nicotiana* diverged from *Physalis* and *Solanum* 30 million years ago and a generation time of 2 years (see text).
24. An *S* lineage was considered trans-generic if it inserted into the *S*-gene genealogy at a position ancestral to an allele found in *Nicotiana* [or *Petunia*, a more distantly related genus in the Solanaceae (*21*)]. The sensitivity of this estimate to uncertainty in the phylogeny was examined by use of the bootstrap. The data were resampled 100 times with replacement, and the number of trans-generic lineages was determined for each replicate.
25. D. Lewis, *Heredity* **5**, 399 (1951).
26. S. Wright, *Biometrics* **16**, 61 (1960).
27. M. D. Lane and M. J. Lawrence, *Heredity* **71**, 596 (1993).
28. S. O'Donnell, M. D. Lane, M. J. Lawrence, *ibid.*, p. 591.
29. G. J. Paxman, *Genetics* **48**, 1029 (1963).
30. N. Mantel, *Biometrics* **30**, 355 (1974).
31. M. K. Uyenoyama, *Genetics* **139**, 975 (1995).
32. M. Nei and L. Jin, *Mol. Biol. Evol.* **6**, 290 (1989); A. L. Hughes and M. Nei, *Proc. Natl. Acad. Sci. U.S.A.* **86**, 958 (1989).
33. S. Kumar, K. Tamura, M. Nei, Molecular Evolutionary Genetics Analysis package (Pennsylvania State University, 1993).
34. B. Xu, J. Mu, D. L. Nevins, P. Grun, T.-h. Kao, *Mol. Gen. Genet.* **224**, 341 (1990).
35. M. K. Saba-El-Leil, S. Rivard, D. Morse, M. Cappadocia, *Plant Mol. Biol.* **24**, 571 (1994).
36. H. Kaufmann, F. Salamini, R. D. Thompson, *Mol. Gen. Genet.* **226**, 457 (1991).
37. J. Royo *et al.*, *Proc. Natl. Acad. Sci. U.S.A.* **91**, 6511 (1994).
38. J. Royo, Y. Kowyama, A. E. Clarke, *Plant Physiol.* **105**, 751 (1994).
39. I. K. Chung *et al.*, *Plant Mol. Biol.* **26**, 757 (1994).
40. A. Kheyr-Pour *et al.*, *Sex. Plant Reprod.* **3**, 88 (1990).
41. Y. J. Ai, D. S. Tsai, T.-h. Kao, *Plant Mol. Biol.* **19**, 523 (1992).
42. K. R. Clark, J. J. Okuley, P. D. Collins, T. L. Sims, *Plant Cell* **2**, 815 (1990).
43. Y. Ai *et al.*, *Sex. Plant Reprod.* **3**, 130 (1990).
44. W. Jost, H. Bak, K. Glund, P. Terpstra, J. J. Beinteme, *Eur. J. Biochem.* **198**, 1 (1991).
45. H. Ide, M. Kimura, M. Arai, G. Funatsu, *FEBS Lett.* **284**, 161 (1991).
46. J. D. Thompson, D. G. Higgins, T. J. Gibson, *Nucleic Acids Res.* **22**, 4673 (1994).
47. J. Felsenstein, Phylip 3.5 (Department of Genetics, University of Washington, Seattle, 1993).
48. Supported by a grant from the Sloan Foundation (A.D.R.), NSF grants DEB-9404386 (A.D.R.), DEB-9306473 (J.R.K.), DEB-9527843 (J.R.K. and A.D.R.), a Hellman Fellowship (J.R.K.), and USPHS grant GM 37841 (M.K.U.). The assistance of the staff of the University of California Philip L. Boyd Deep Canyon Reserve is gratefully acknowledged.

15 March 1996; accepted 31 May 1996

Forskolin Stimulation of Water and Cation Permeability in Aquaporin1 Water Channels

Andrea J. Yool, W. Daniel Stamer, John W. Regan

Aquaporin1, a six–transmembrane domain protein, is a water channel present in many fluid-secreting and -absorbing cells. In *Xenopus* oocytes injected with aquaporin1 complementary RNA, the application of forskolin or cyclic 8-bromo- adenosine 3′,5′-monophosphate increased membrane permeability to water and triggered a cationic conductance. The cationic conductance was also induced by direct injection of protein kinase A (PKA) catalytic subunit, reduced by the kinase inhibitor H7, and blocked by $HgCl_2$, an inhibitor of aquaporin1. The cationic permeability of the aquaporin1 channel is activated by a cyclic adenosine monophosphate–dependent mechanism that may involve direct or indirect phosphorylation by PKA.

Lipid bilayers have an inherently low water permeability, an attribute that benefits life in aqueous and terrestrial environments. In specialized cells, water permeability is enhanced by the expression of aquaporins, integral membrane proteins that regulate osmotically driven transmembrane water fluxes (*1*). The primary sequences of aquaporins predict six transmembrane domains and internal NH_2- and COOH-terminal domains (*2*). This structural motif is similar to that of other channels and transporters (*3*).

In *Xenopus* oocytes, expression of complementary RNA (cRNA) encoding human aquaporin1 (CHIP28) confers an increased osmotic water permeability (*4*). Aquaporins 2 and 5 have consensus sites for the adenosine 3′,5′-monophosphate (cAMP)–dependent PKA (*5*). Aquaporin2, the vasopressin-regulated water channel, shows a cAMP-dependent increase in water permeability when expressed in *Xenopus* oocytes (*6*). In contrast, aquaporins 1 and 3 lack typical consensus sequences for phosphorylation by PKA and are thought to be constitutively active.

Voltage-clamp studies of *Xenopus* oocytes with aquaporin1 cRNA provide no evidence for ionic permeability (*4*, *7*). We also have found that the unstimulated aquaporin1 channel shows no evidence of net ionic flux. However, after treatment with forskolin, which increases production of cAMP by adenylyl cyclase, the rate of osmotically driven water uptake in aquaporin1-injected oocytes (*8*) was increased (Fig. 1). Swelling was quantitated by videomicroscopy after exposure of an oocyte to hypotonic saline (100-mOsm gradient). Oocytes incubated for 15 min in isotonic saline containing 10 μM forskolin showed the greatest subsequent rate of swelling in hypotonic saline. Ethanol (0.1%), used for dissolving forskolin, had no effect alone on swelling. Unstimulated oocytes expressing aquaporin1 showed an intermediate rate of swelling; their initial swelling rate was decreased 66% by $HgCl_2$ (100 μM), a blocker of water channels (*9*, *10*). Water-injected control oocytes showed a low swelling rate that was unaffected by forskolin. Calculated coef-

A. J. Yool, Departments of Physiology and Pharmacology, University of Arizona, Tucson, AZ 85724–5051, USA. W. D. Stamer, Department of Pharmacology and Toxicology, University of Arizona, Tucson, AZ 85721, USA. J. W. Regan, Department of Pharmacology and Toxicology and Department of Physiology, Program in Neuroscience, University of Arizona, Tucson, AZ 85721, USA.

ficients of osmotic water permeability (P_f) (*11*) were 49 ± 2 μm/s (mean ± SE, n = 5) for forskolin-stimulated aquaporin1-injected oocytes, 30 ± 7 μm/s (n = 5) for unstimulated aquaporin1-injected oocytes, and 1.9 ± 1 μm/s (n = 3) for water-injected oocytes.

The forskolin-stimulated increase of water permeability led us to reevaluate the ionic permeation properties of this channel (*12*). We measured currents by two-electrode voltage clamp under initial conditions (Fig. 2, A and E) and 15 min after forskolin (10 μM) treatment in isotonic NaCl saline (Fig. 2, B and F). Water-injected oocytes showed no appreciable change in conductance. Oocytes expressing aquaporin1 showed a large increase in conductance. To remove leak and capacitance, we subtracted traces for the initial response from traces after forskolin; the difference current represents the forskolin-activated conductance, which was negligible in water-injected controls but large in aquaporin1-injected oocytes (Fig. 2, C and G). The difference current was not affected by $HgCl_2$ (20 μM) in water-injected controls (Fig. 2, C and D), but was reduced by 54% in aquaporin1-injected oocytes (Fig. 2, G and H), indicating that the forskolin-stimulated ion conductance probably is mediated by aquaporin1 channels. The inhibition by $HgCl_2$ was similar at 20 and 100 μM, but higher concentrations (>1 mM) appeared detrimental to all oocytes and caused rapid degradation of membrane integrity. To rule out the possibility that the forskolin-stimulated ionic fluxes represented a Hg-sensitive endogenous current, we tested the Hg-insensitive aquaporin1 mutant C189S (*10*); in this instance, the forskolin-stimulated conductance was not blocked by Hg^{2+} (*13*). Thus, an endogenous current appears not to account for the forskolin-stimulated ionic response.

The current-voltage relation of the forskolin-stimulated ionic flux is linear (Fig. 3). The reversal potential in NaCl saline (−16.6 ± 1.4 mV; mean ± SE, n = 17) indicated that Cl^- or mixed cations were the charge carriers (*12*). Equimolar substitution of 60 mM Cl^- with gluconate did not shift the reversal potential of the forskolin-stimulated current (−15.2 ± 1.2 mV, n = 8), indicating that Cl^- is not directly involved. Substitutions of Cl^- by acetate or aspartate also yielded reversal potentials near −14 mV (*13*). In contrast, equimolar substitution of Na^+ with K^+ yielded a more positive reversal potential (−10.3 ± 2.8 mV, n = 5), also seen with Cs^+. Substitution of Na^+ by tetraethylammonium (TEA) yielded a more negative reversal potential (−39.6 ± 6.0 mV, n = 6). The reversal potential was not appreciably affected at pH 6.3 or 8.3. Thus, under physiological conditions, cations appear to be the primary current carriers in cAMP-activated aquaporin1 channels. Endogenous oocyte currents in water-injected oocytes had a reversal potential in NaCl saline of −17.6 ± 2.5 mV (mean ± SE, n = 12). The substitution of gluconate for 60 mM Cl^- gave a reversal potential of −1.1 ± 0.9 mV (n = 9), showing that the endogenous current is dependent on Cl^-. In TEACl saline, the reversal potential was −32.3 ± 2.3 mV (n = 4), also implicating a cationic component. Thus, the endogenous current differs from the forskolin-stimulated aquaporin1 current in several ways: it is smaller in amplitude, dependent in part on Cl^-, insensitive to Hg^{2+} at ≤100 μM, and is not affected by forskolin.

The macroscopic conductance, measured as the slope of the linear current-voltage relation, increased about six- to eightfold after forskolin treatment of aquaporin1-injected oocytes (Table 1). Application of cyclic 8-bromo-adenosine 3′,5′-monophosphate (8Br-cAMP, 1 mM in NaCl saline) also resulted in an increase in conductance (3.98 ± 0.83–fold increase; mean ± SE, n = 4) after 10 to 15 min of treatment. Initial ionic conductances were not substantially different between water- and aquaporin1-injected oocytes (Fig. 2 and Table 1), which may explain why ionic permeability has not been noted previously. Ionic permeability in aquaporin1 channels appears to require intracellular signaling, whereas water permeability is a feature of both the stimulated and unstimulated states.

Injection of the catalytic subunit of PKA into aquaporin1-expressing oocytes rapidly induced the cationic current (Fig. 4A). The

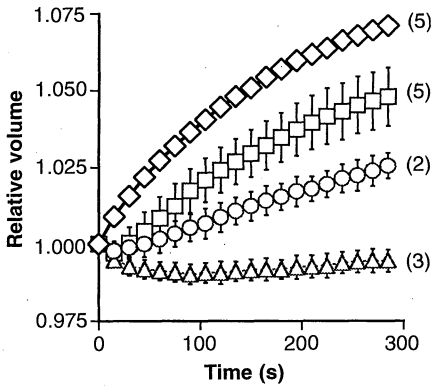

Fig. 1. Forskolin-stimulated increase in osmotic water permeability of oocytes expressing aquaporin1. Osmotic swelling was monitored at 15-s intervals for oocytes exposed to 100-mOsm hypotonic saline at time zero (*8*). Oocytes injected with aquaporin1 cRNA were first incubated for 15 min in isotonic saline alone (□), for 15 min with forskolin (10 μM) (◇), or for 5 min in 100 μM $HgCl_2$ (○) before exposure to hypotonic saline. Control oocytes were injected with water (△) and incubated for 15 min in isotonic saline before exposure to hypotonic saline. Data are shown as the mean ± SE; the number of oocytes is indicated in parentheses. Similar results were obtained in five separate experiments with oocytes from different frogs.

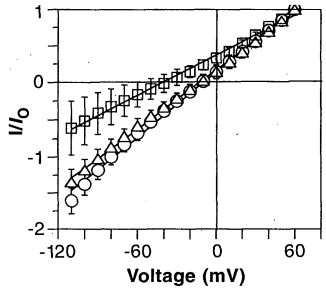

Fig. 3. Ionic dependence of the forskolin-stimulated current in oocytes expressing aquaporin1. Ionic selectivity was evaluated from the current-voltage relations of the forskolin-stimulated peak current amplitudes, plotted as mean ± SD for isotonic external salines (*12*) containing NaCl (○) (n = 16), K gluconate with NaCl (△) (n = 7), or TEACl (□) (n = 6). I, current.

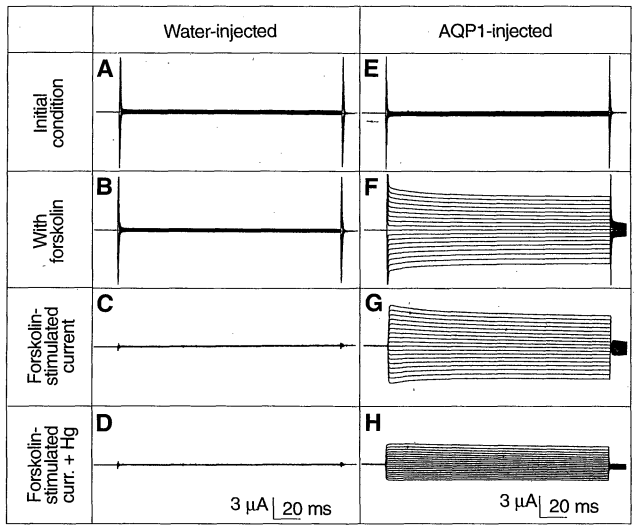

Fig. 2. Ionic conductance induced by forskolin in aquaporin1 (AQP1)-injected but not in water-injected oocytes. Total currents in isotonic NaCl saline were recorded before treatment (**A** and **E**) and 15 min after exposure to forskolin at 10 μM (**B** and **F**). Net forskolin-stimulated currents (**C** and **G**) were obtained by subtracting initial traces from those after forskolin treatment. The forskolin-stimulated current was reduced by 20 μM $HgCl_2$ (**H**). Water-injected oocytes were not affected (**D**). For two-electrode voltage-clamp recordings, voltage steps from +60 to −110 mV were used in increments of 10 mV from a holding potential of −30 mV (*12*).

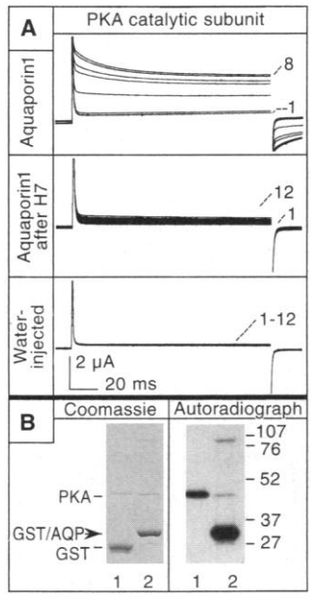

Fig. 4. Activation of the aquaporin1 ionic current and phosphorylation of a fusion protein of aquaporin1 by the catalytic subunit of protein kinase A. (**A**) Injection of the catalytic subunit of protein kinase A (PKA, ~1 U total in 10 nl) was done on-line during repeated voltage steps (to +40 mV at 5-s intervals over 8 to 12 min) in oocytes expressing aquaporin1 channels and in water-injected controls (top three panels). Aquaporin1-injected oocytes were also tested after 2 to 3 hours incubation with kinase inhibitor H7 (10 μM). Traces are shown at 1-min intervals (times are indicated at right of traces). The holding potential was −30 mV; traces shown are not subtracted for leak and capacitance. (**B**) The Coomassie-stained SDS-polyacrylamide gel (left) shows the positions of GST (lane 1, 27 kD) and the aquaporin1 COOH-terminal fusion protein (GST/AQP; lane 2, 31 kD). The corresponding autoradiograph (right) shows phosphorylation by [γ-^{32}P]ATP (14 μM) of the fusion protein (GST/AQP, lane 2) but not GST alone (lane 1) after 10 min with 60 U of PKA catalytic subunit (*18*). Molecular sizes are indicated on the right (in kilodaltons).

Table 1. Conductance properties of water-injected and aquaporin1-injected oocytes. Total conductance represents values before treatment of oocytes with forskolin (10 μM, 12 to 15 min). Data are shown as the mean ± SE, and the number of oocytes analyzed is given in parentheses. Conductance was measured from the linear slope of the current-voltage relation. Values for percentage block by Hg^{2+} are combined for NaCl and K gluconate conditions, which showed no significant difference ($P > 0.10$; Student's t test).

Conductance property	Water-injected (*n*)	Aquaporin1-injected (*n*)
Total initial conductance (μA/V)		
NaCl	2.86 ± 0.6 (14)	8.63 ± 2.0 (16)
K gluconate	3.82 ± 1.0 (9)	4.53 ± 0.5 (8)
TEACl	1.00 ± 0.04 (4)	3.13 ± 1.1 (4)
Increase after forskolin treatment (%)		
NaCl	113 ± 9 (12)	633 ± 142 (11)
K gluconate	150 ± 17 (9)	814 ± 94 (8)
TEACl	121 ± 10 (4)	666 ± 113 (4)
Inhibition of forskolin-activated conductance by $HgCl_2$ (%)	≤0 (22)	55.7 ± 3.8 (13)

effect reached maximum amplitude by 7 to 8 min after injection and was reduced by treatment with the kinase inhibitor H7. Treatment with H7 also blocked the similar effect caused by direct injection of 8Br-cAMP (*13*). Water-injected control oocytes showed no response to injected catalytic subunit or to 8Br-cAMP. Because aquaporin1 lacks a preferred consensus sequence for phosphorylation by PKA, the stimulation of conductance may be a consequence of phosphorylation at an atypical site (*14*). Incubation of a fusion protein containing the COOH-terminus of aquaporin1 with the catalytic subunit of PKA resulted in labeling with ^{32}P, suggesting that direct phosphorylation may occur (Fig. 4B); however, indirect phosphorylation of another protein is also possible. Activation by cyclic nucleotide binding (*15*) is unlikely to be a primary mechanism because the effect of 8Br-cAMP injection was antagonized by treatment with H7.

We conclude that cAMP-mediated stimulation induces aquaporin1 channels to become more permeant to water and to acquire cationic permeability. The regulation of permeability through a cAMP-dependent mechanism has potential relevance in many cells that express aquaporin1, including those in eye that regulate intraocular pressure (*16*) and in capillary endothelia of cardiac and skeletal muscle (*17*). The cAMP-dependent increase in permeability to water and cations suggests that aquaporin1 channels could contribute to aspects of receptor-mediated signaling as well as regulated water fluxes.

REFERENCES AND NOTES

1. P. Agre *et al.*, *Am. J. Physiol.* **265**, F463 (1993).
2. G. M. Preston and P. Agre, *Proc. Natl. Acad. Sci. U.S.A.* **88**, 11110 (1991).
3. L. Y. Jan and Y. N. Jan, *Cell* **69**, 715 (1992).
4. G. M. Preston, T. P. Carroll, W. B. Guggino, P. Agre, *Science* **256**, 385 (1992).
5. S. Raina, G. M. Preston, W. B. Guggino, P. Agre, *J. Biol. Chem.* **270**, 1908 (1995).
6. M. Kuwahara *et al.*, *ibid.*, p. 10384.
7. R. Zhang *et al.*, *J. Cell Biol.* **120**, 359 (1993).
8. Aquaporin1 wild-type and mutant C189S cDNA was provided by P. Agre, and cRNA was synthesized in vitro. Oocytes from *Xenopus laevis* were obtained by surgery and prepared as described [W. Zagotta, T. Hoshi, R. Aldrich, *Proc. Natl. Acad. Sci. U.S.A.* **86**, 7243 (1989)]. Oocytes were injected with 50 nl of water with or without 1 ng of aquaporin1 cRNA and incubated for ≥2 days at 18°C in ND96 medium [96 mM NaCl, 2.0 mM KCl, 1.8 mM $CaCl_2$, 1.0 mM $MgCl_2$, 5 mM Hepes (pH 7.6)] to allow expression. Hypotonic saline was made with ND96 saline diluted with an equal volume of water to ~100 mOsm. Cross-sectional areas were analyzed (Image1; Universal Imaging, West Chester, PA) for the rate of volume change with time.
9. R. I. Macey, *Am. J. Physiol.* **246**, C195 (1984).
10. G. M. Preston, J. S. Jung, W. B. Guggino, P. Agre, *J. Biol. Chem.* **268**, 17 (1993).
11. J. Fischbarg *et al.*, *Proc. Natl. Acad. Sci. U.S.A.* **86**, 8397 (1989). Osmotic water permeability (P_f) was calculated from initial volume change as $P_f = [V_o \times d(V/V_o)/dt]/[S \times V_w(Osm_{in} - Osm_{out})]$, where initial cell volume $V_o = 9 \times 10^{-4}$ cm^3, initial oocyte surface area S = 0.0045 cm^2, and the volume of water V_w = 18 cm^3/mol.
12. Electrophysiological recordings were done with isosmotic NaCl saline [100 mM NaCl, 2 mM KCl, 4.3 mM $MgCl_2$, and 5 mM Hepes (pH 7.3)] or isosmotic test salines made by substitution of 100 mM NaCl with either 60 mM K gluconate with 40 mM NaCl, or 100 mM TEACl. Ca^{2+} was omitted to minimize the Ca^{2+}-dependent Cl^- current [M. Barish, *J. Physiol. London* **342**, 309 (1983)]. For two-electrode voltage clamp at room temperature, electrodes (0.5 to 3 MΩ) containing 3M KCl were used. Healthy oocytes were selected by resting potentials (−25 to −40 mV) and low initial holding currents (usually 0 to −50 nA at −30 mV) and consistently yielded small stable currents in the unstimulated state. Unhealthy oocytes (regardless of injection regime) had depolarized resting potentials, high initial holding currents, and large unstable leak currents that were insensitive to forskolin or Hg^{2+}. Sonicated $HgCl_2$ stock (100 mM) was diluted in saline for perfusion at the final concentration. Data recorded by GeneClamp were stored to computer hard disk and analyzed with pClamp (Axon Instruments).
13. A. J. Yool, W. D. Stamer, J. W. Regan, unpublished data.
14. X.-B. Chang *et al.*, *J. Biol. Chem.* **268**, 11304 (1993); D. P. Rich *et al.*, *ibid.*, p. 20259.
15. A. Brüggemann, L. A. Pardo, W. Stühmer, O. Pongs, *Nature* **365**, 445 (1993); U. B. Kaupp, *Trends Neurosci.* **14**, 150 (1991).
16. W. D. Stamer, R. W. Snyder, B. L. Smith, P. Agre, J. W. Regan, *Invest. Ophthalmol. Visual. Sci.* **35**, 3867 (1994).
17. S. Nielsen, B. L. Smith, E. I. Christensen, P. Agre, *Proc. Natl. Acad. Sci. U.S.A.* **90**, 7275 (1993).
18. A fusion protein of glutathione-S-transferase (GST) and the 38–amino acid COOH-terminal portion of aquaporin1 (GST/AQP; molecular weight, 31,300) was made as described [W. D. Stamer, R. Seftor, R. Snyder, J. Regan, *Curr. Eye Res.* **14**, 1095 (1995)]. About 20 μg of either GST or GST/AQP was incubated (10 min, 37°C) with 60 U of PKA catalytic subunit (bovine heart, Promega) and 14 μM [^{32}Pγ]ATP (2.9 Ci/mmol, NEN-Dupont) in 50 μl of buffer containing 5 mM tris (pH 7.5 at 23°C), 5 mM $MnCl_2$, 75 mM $MgCl_2$, and 1 mM dithiothreitol. After addition of 2 mM EDTA, proteins were precipitated with 5% trichloroacetic acid and separated by electrophoresis on a 12% polyacrylamide gel stained with Coomassie blue, dried, and subjected to autoradiography (16 hours; X-OMAT, Kodak).

19. We thank S. Wright for helpful discussions and help with imaging. The following grant support is acknowledged: American Heart Association Arizona Affiliate AZFG-20-93 (A.J.Y.), Pharmaceutical Research Manufacturers America Foundation Inc. (W.D.S.) and EY09355 (J.W.R.), Glaucoma Foundation 95 (J.W.R.), Allergan 4 (J.W.R.), and National Science Foundation IBN94-07997 (S. Wright).

27 February 1996; accepted 9 July 1996